Oxidative-Addition of Organic Monochloro Derivatives to Dinuclear Iridium Complexes: The Detection of Tautomeric Equilibria and Their Implications on the Reactivity

Cristina Tejel, Miguel A. Ciriano,* José A. López, Fernando J. Lahoz, and Luis A. Oro*

Departamento de Química Inorgánica, Instituto de Ciencia de Materiales de Aragón, Universidad de Zaragoza-CSIC, E-50009 Zaragoza, Spain

Received April 13, 2000

Reactions of $MeCOCH_2Cl$, $MeCO_2CH_2Cl$, and (−)-methyl(S)-2-chloropropionate with [{Ir(μ-Pz)($CNBu^t$)$_2$}$_2$] (Pz = pyrazolate, **1**) gave the metal−metal bonded diiridium(II) complexes [($CNBu^t$)$_2$(Cl)Ir(μ-Pz)$_2$Ir(η^1-CH_2R)($CNBu^t$)$_2$] (R = COMe (**2**), CO_2Me (**3**)) and the two enantiomers of [($CNBu^t$)$_2$(Cl)Ir(μ-Pz)$_2$Ir(η^1-CH(Me)CO_2Me)($CNBu^t$)$_2$] (**4**). Similar reactions of **1** with equimolar amounts of benzyl chloride and allyl chloride rendered [($CNBu^t$)$_2$(Cl)Ir(μ-Pz)$_2$Ir(η^1-CH_2R)($CNBu^t$)$_2$] ((R = Ph (**5**), CH=CH_2 (**7**)), which were found to be the metal−metal bonded complexes in the solid state, but in equilibrium with the mixed-valence Ir(I)−Ir(III) complexes [($CNBu^t$)$_2$Ir(μ-Pz)$_2$Ir(Cl)(η^1-CH_2R)($CNBu^t$)$_2$] in solution. Replacement of chloride by iodide in **5** affords only the diiridium(II) complex [($CNBu^t$)$_2$(I)Ir(μ-Pz)$_2$Ir(η^1-CH_2-Ph)($CNBu^t$)$_2$] (**6**). Complexes **5** and **7** reacted further with a second molar equivalent of chloro derivative to render dialkyldiiridium(III) complexes [{Ir(μ-Pz)(η^1-CH_2R)($CNBu^t$)$_2$}$_2$(μ-Cl)]Cl, ((R = Ph (**8**), CH=CH_2 (**10a**)), while those showing a single static species in solution (**2**−**4** and **6**) were inactive. The reaction of **7** with allyl chloride gave also the isomer [($CNBu^t$)$_2$-(Cl)Ir(η^1,η^2-$CH_2CH{=}CH_2$)(μ-Pz)$_2$Ir(η^1-allyl)($CNBu^t$)$_2$]Cl (**10b**), in which one allyl group bridges the two iridium atoms in an unsymmetrical fashion. This complex isomerizes into the thermodynamic product [{Ir(μ-Pz)(η^1-allyl)($CNBu^t$)$_2$}$_2$(μ-Cl)]Cl, an stereoisomer of **10a**. The structures of **10b** and **5** were solved by single-crystal X-ray diffraction methods.

Introduction

Oxidative-addition reactions of haloalkanes to binuclear iridium(I) complexes follow a common pattern yielding diiridium(II) metal−metal bonded compounds. The two fragments R and X become systematically located *trans* to the Ir−Ir bond in the reactions with the most usual haloalkanes, namely, MeI and CH_2I_2, with independence of the type of bridging ligands in the starting complexes: pyrazolate,[1] *tert*-butylthiolate,[2] diamidonaphthalene,[3] pyridine-2-thiolate,[4] 7-azaindolate,[5] or mixed ligands Pz, SBu^t.[6] The few exceptions to this pattern are the addition of MeI to [{Ir(μ-NHPhMe)-$(CO)_2$}$_2$][7] and [$Ir_2(CO)_2$(μ-PPh_2)(μ-PNNP)],[8] resulting in mixed-valence Ir(I)−Ir(III) compounds.

A further oxidative-addition of haloalkane to these diiridium(II) complexes, which would cleavage the iridium−iridium bond, has not been described. In this way, access to alkyl diiridium(III) dinuclear complexes through oxidative-addition reactions is restricted either by the stability of the Ir−Ir bond or by the lack of an easy reaction pathway for a further reaction. However, few methylene-bridged diiridium(III) complexes become accessible either directly by reaction[9] with CH_2I_2 or through a thermal oxidative-isomerization reaction[3,6,10] of iodomethyldiiridium(II) complexes. These observations show a relative inertness of dinuclear d^7−d^7 iridium systems with diolefin, carbonyl, and phosphine ligands to react with haloalkanes. Exceptions to this general behavior were exemplified by the compounds [$(L)_2$(Me)Ir(μ-Pz)$_2$(μ-I)Ir(Me)($CNBu^t$)$_2$]I (L = $CNBu^t$, 1/2 cod), coming unexpectedly from the double oxidative-addition of CH_3I to the complexes [$(L)_2$Ir(μ-Pz)$_2$Ir-($CNBu^t$)$_2$].[11]

Very few reactions of diiridium(I) compounds with chloroalkanes have been reported so far.[5,12] They re-

(1) (a) Oro, L. A.; Sola, E.; López, J. A.; Torres, F.; Elduque, A.; Lahoz, F. J. *Inorg. Chem. Commun.* **1998**, *1*, 64. (b) Bushnell, G. W.; Fjeldsted, D. O. K.; Stobart, S. R.; Wang, J. *Organometallics* **1996**, *15*, 3785, and references therein.

(2) El Amane, M.; Maisonnat, A.; Dahan, F.; Poilblanc, R. *New. J. Chem.* **1988**, *12*, 661.

(3) Fernández, M. J.; Modrego, J.; Lahoz, F. J.; López, J. A.; Oro, L. A. *J. Chem. Soc., Dalton Trans.* **1990**, 2587.

(4) Ciriano, M. A.; Viguri, F.; Oro, L. A.; Tiripicchio, A.; Tiripicchio-Camellini, M. *Angew. Chem., Int. Ed. Engl.* **1987**, *26*, 444.

(5) Ciriano, M. A.; Pérez-Torrente, J. J.; Oro, L. A. *J. Organomet. Chem.* **1993**, *445*, 273.

(6) Pinillos, M. T.; Elduque, A.; López, J. A.; Lahoz, F. J.; Oro, L. A. *J. Chem. Soc., Dalton Trans.* **1991**, 1391.

(7) Kolel-Veetil, M. K.; Rheingold, A. L.; Ahmed, K. J. *Organometallics* **1993**, *12*, 3439.

(8) Schenck, T. G.; Milne, C. R. C.; Sawyer, J. F.; Bosnich, B. *Inorg. Chem.* **1985**, *24*, 2338.

(9) El Amane, M.; Maisonnat, A.; Dahan, F.; Pince, R.; Poilblanc, R. *Organometallics* **1985**, *4*, 773.

(10) Brost, R. D.; Stobart, S. R. J. *Chem. Soc., Chem. Commun.* **1989**, 498.

(11) Tejel, C.; Ciriano, M. A.; Edwards, A. J.; Lahoz, F. J.; Oro, L. A. *Organometallics* **1997**, *16*, 45.

(12) Caspar, J. V.; Gray, H. B. *J. Am. Chem. Soc.* **1984**, *106*, 3029.

10.1021/om000314v CCC: $19.00
Publication on Web 10/28/2000

quired visible or UV light irradiation to produce the oxidative-addition of the chloroalkane leading to metal−metal bonded complexes containing "Cl−Ir(II)−Ir(II)−X" (X = R, Cl) frameworks.

In this paper we describe the reactivity of the complex $[\{Ir(\mu\text{-Pz})(CNBu^t)_2\}_2]$ with several chloroalkanes to give either metal−metal bonded diiridium(II) compounds or bis(alkyl)diiridium(III) complexes. In addition, we discuss the reasons for this differential behavior based on the intermediacy of unusual active mixed-valence Ir(I)−Ir(III) species in solution. Part of this work has been previously communicated.[13]

Results

Metal−Metal Bonded Dinuclear Iridium Pyrazolate Complexes. The dinuclear complex $[\{Ir(\mu\text{-Pz})(CNBu^t)_2\}_2]$ (Pz = pyrazolate, **1**) reacted with $MeCOCH_2Cl$ and $MeCO_2CH_2Cl$ in benzene and in the dark to give $[\{Ir(\mu\text{-Pz})(CNBu^t)_2\}_2(Cl)(\eta^1\text{-}CH_2R)]$ (R = COMe, **2**; CO_2Me, **3**) (Scheme 1). Both complexes were found to be single and static in solution by ^1H NMR, with equivalent pyrazolate groups. The bonding of the RCH_2- group to the iridium through the CH_2 carbon was evidenced by a high-field resonance in the $^{13}C\{^1H\}$ NMR spectra. Further information about their structures was given by NOE difference spectra (Figure 1), which revealed the close proximity of the RCH_2- group and the H^3 protons of the pyrazolate rings. These data agree with the two structures shown in Chart 1: the diiridium(II) species (**A**) containing the chloride and CH_2R groups *trans* to the metal−metal bond and the mixed-valence Ir(I)−Ir(III) complex (**B**) containing these fragments in a *trans* disposition on one iridium center, with the RCH_2- ligand at the *exo* position. However, complexes **2** and **3** must be formulated as the metal−metal bonded species, **A**, since their variable (low and high) temperature ^1H NMR spectra in several solvents did not reveal the presence of any fluxional process, which should be expected for the facile inversion[14] of the six-membered ring "$Ir(N-N)_2Ir$" in the species **B**. Indeed, related Rh complexes of this type were found to exist as two interconverting conformers,[15] for which the major species were the *endo* conformer, a stereochemistry and equilibria not found for complexes **2** and **3**.

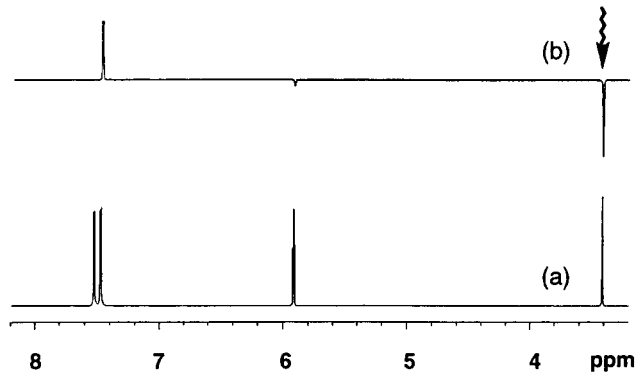

Figure 1. NOE difference spectra of $[\{Ir(\mu\text{-Pz})(CNBu^t)_2\}_2(Cl)(\eta^1\text{-}CH_2COMe)]$ (**2**) in acetone-d_6 upon irradiation at the CH_2 protons: (a) normal spectrum, (b) difference spectrum.

Scheme 1

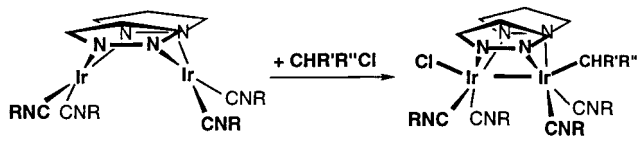

R = Bu^t; R' = H, R" = COMe (2), CO_2Me (3); R' = Me, R" = CO_2Me (4)

Chart 1

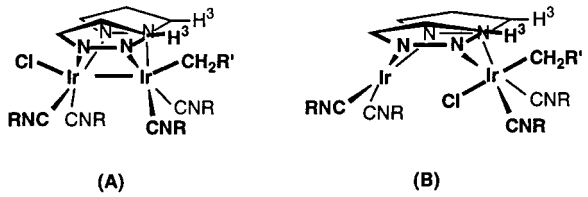

R = Bu^t; R' = COMe, CO_2Me

The reaction of **1** with the simplest chiral chloro derivative (−)-methyl(S)-2-chloropropionate, $MeCO_2CH(Me)Cl$, provided some information on the mechanism involved, at least, for this reaction. The product, $[(CNBu^t)_2(Cl)Ir(\mu\text{-Pz})_2Ir\{CH(Me)CO_2Me\}(CNBu^t)_2]$ (**4**), was found to be a single and nonfluxional species in C_6D_6. Spectroscopic NMR data indicated the bonding of the $CH(Me)CO_2Me$ group through the secondary carbon to iridium. In addition, preliminary X-ray diffraction[16] studies on a single crystal of **4** confirmed the location of the Cl and $CH(Me)CO_2Me$ groups at different iridium centers, both *trans* to the iridium−iridium bond. Measurements of the rotatory specific power of the crude of the reaction and of the isolated solid **4** showed a value close to zero, evidencing the presence of a racemic mixture. Accordingly, the two enantiomers were observed by ^1H NMR upon addition of $Eu(hfc)_3$ {hfc = 3-(heptafluoropropylhydroxymethylene)-(+)-camphorato}. As only the S_N2 profile produces inversion of the configuration of the asymmetric carbon (Walden inversion), either a radical or an S_N1 mechanism (unlikely in benzene) operates for the addition of the chiral chloroderivative to **1**.

Equilibria between Dinuclear Iridium Pyrazolate Complexes. Complex **1** easily reacted with 1 molar equiv of $PhCH_2Cl$ in benzene to give **5**, which was isolated as long orange needles. A recently reported X-ray diffraction study[13] showed that **5** is the diiridium(II) complex $[(CNBu^t)_2(Cl)Ir(\mu\text{-Pz})_2Ir(\eta^1\text{-}CH_2Ph)(CNBu^t)_2]$ (**5a**), with an Ir−Ir bond in the solid state (Figure 2). However, solutions of monocrystals of **5** showed the presence of two species in the ^1H NMR spectrum (Figure 3a). Both species have identical formulation $[\{Ir(\mu\text{-Pz})(CNBu^t)_2\}_2(Cl)(\eta^1\text{-}CH_2Ph)]$ and symmetry (C_s); the major species (82%) contains the $PhCH_2$ group close to the H^3 protons of the pyrazolate rings, as shown by positive cross-peaks between these resonances in the phase-sensitive NOESY spectrum at room temperature (Figure 4a), while these protons are far away in the minor species. Accordingly, the major species could be **5a** or **5c** (Scheme 2), while the minor one is the Ir(III)−Ir(I)complex $[(CNBu^t)_2Ir(\mu\text{-Pz})_2Ir(Cl)(\eta^1\text{-}CH_2Ph)(CNBu^t)_2]$,

(13) Tejel, C.; Ciriano, M. A.; López, J. A.; Lahoz, F. J.; Oro, L. A. *Organometallics* **1998**, *17*, 1449.
(14) Tejel, C.; Villoro, J. M.; Ciriano, M. A.; López, J. A.; Eguizábal, E.; Lahoz, F. J.; Bakhmutov, V. I.; Oro, L. A. *Organometallics* **1996**, *15*, 2967.
(15) Tejel, C.; Ciriano, M. A.; Edwards, A. J.; Lahoz, F. J.; Oro, L. A. *Organometallics* **2000**, *19*, 4968.
(16) Edwards, A. J.; Clegg, W. Private communication.

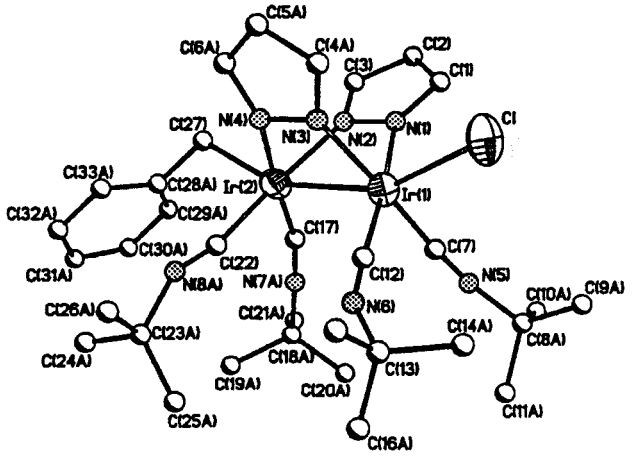

Figure 2. Structure of the diiridium(II) complex $[(CNBu^t)_2(Cl)Ir(\mu\text{-}Pz)_2Ir(\eta^1\text{-}CH_2Ph)(CNBu^t)_2]$ (**5a**).

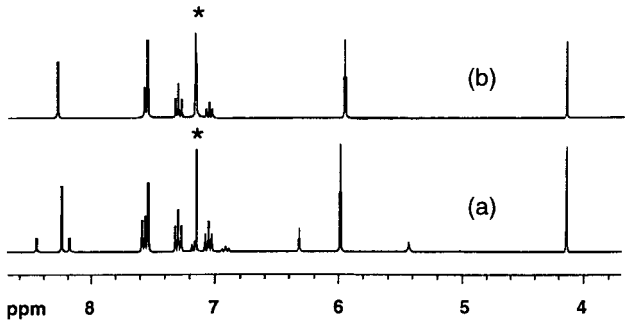

Figure 3. ^{1}H NMR spectra of **5** showing the two species **5a** and **5b** (a) and of **6** (b) in C_6D_6. The astrerisk denotes the signal of the nondeuterated solvent.

Scheme 2

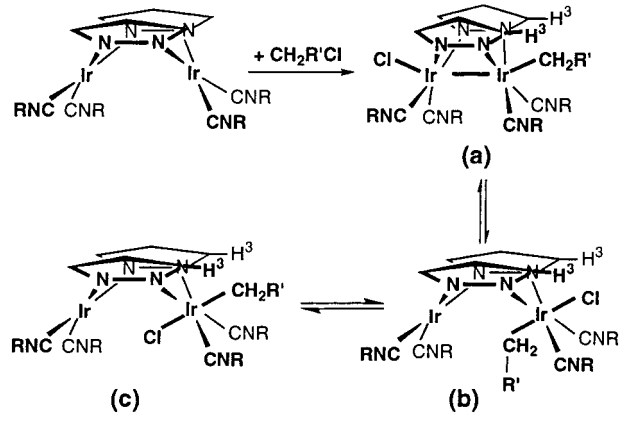

with the $PhCH_2$ group in the pocket of the complex (**5b**, Scheme 2).

A relevant spectroscopic difference between **5a**/**c** and **5b** is the chemical shift for the benzyl protons, which are separated 1.3 ppm in the ^{1}H NMR spectrum. According to previous observations,[15] the low-field shifted resonance corresponds to the compound with the RCH_2− group situated in the pocket of the complex, which indeed agrees with the lack of NOE between the CH_2 and pyrazolate protons for the minor species **5b**. The most remarkable feature of complex **5** is that the two species observed in solution are in chemical equilibrium, detected by the presence of negative cross-peaks between all pairs of resonances of both complexes in the phase-sensitive ROESY spectrum carried out at 313 K (Figure 4b). Variable-temperature ^{1}H NMR spectra of solutions of the orange needles in toluene-d_8 indicated that this interconversion is a high-energy process, since only line-broadening effects were detected at 378 K. As a conformational equilibrium between **5b** and **5c** is expected to be a low-energy process,[15] the main species in the equilibrium needs to be **5a**, the species characterized in the solid state. Replacement of chloride by iodide on reacting **5** with potassium iodide in acetone gave $[(CNBu^t)_2(I)Ir(\mu\text{-}Pz)_2Ir(\eta^1\text{-}CH_2Ph)(CNBu^t)_2]$ (**6**), which was found to be the diiridium(II) complex with a metal−metal bond as the single species in solution (Figure 3b). Therefore, the replacement of the chloride by iodide in **5** shifts the equilibrium to the diiridium(II) species.

A second example of such equilibria in dinuclear complexes was found for $[\{Ir(\mu\text{-}Pz)(CNBu^t)_2\}_2(Cl)(\eta^1\text{-}CH_2CH{=}CH_2)]$ (**7**), obtained from the reaction of **1** with 1 molar equiv of allyl chloride in benzene. In this case, the two species were in a 1:10 ratio, the main species being the metal−metal bonded complex $[(CNBu^t)_2(Cl)Ir(\mu\text{-}Pz)_2Ir(\eta^1\text{-}CH_2CH{=}CH_2)(CNBu^t)_2]$ (**7a**), while the minor one was $[(CNBu^t)_2Ir(\mu\text{-}Pz)_2Ir(Cl)(\eta^1\text{-}CH_2CH{=}CH_2)(CNBu^t)_2]$ (**7b**), analogous to **5b**. These species are in chemical equilibrium, evidenced by magnetization transfer techniques.

Compounds **2**−**7** could be classified into two types, namely, those compounds that exist in solution as a single static species with an iridium−iridium bond (complexes **2**−**4** and **6**) and those for which the metal−metal bonded species is in equilibrium with the mixed-valence Ir(I)−Ir(III) complexes (**5** and **7**). While complexes **2**−**4** and **6** were found to be unable to react further, even in an excess of substrate, complexes **5** and **7** reacted with a second molar equivalent of RCH_2Cl. Thus, the diiridium(III) complexes $[(CNBu^t)_2(\eta^1\text{-}CH_2Ph)Ir(\mu\text{-}Pz)_2(\mu\text{-}Cl)Ir(\eta^1\text{-}CH_2R)(CNBu^t)_2]Cl$ (R = CH_2Ph, **8**; CO_2Me, **9**) were obtained by reacting **5** with $PhCH_2Cl$ and $MeCO_2CH_2Cl$, respectively, in the dark. The oxidation of both iridium centers can be followed by the shift to higher frequencies of ν(CN) in their IR spectra, as a consequence of the different σ-donation of the isocyanide ligands. The experimental data support folded structures, containing two pyrazolate and a chloride as bridging ligands. The two organic fragments were *trans* to the chloride bridging ligand and *cis* to both pyrazolate rings, which was definitively confirmed by NOE experiments. However, it is noteworthy that complex **5** does not react with the secondary alkyl chloride $MeCO_2CH(Me)Cl$ under identical conditions.

Complex **7** reacted with 1 molar equiv of $CH_2{=}CHCH_2Cl$, yielding two diiridium(III) complexes of formula $[\{Ir(\mu\text{-}Pz)(CNBu^t)_2\}_2(Cl)(CH_2CH{=}CH_2)_2]Cl$ (**10**). The minor product (15%), characterized by multinuclear NMR spectroscopy, corresponds to the static bridging chloride complex $[\{Ir(\mu\text{-}Pz)(\eta^1\text{-}CH_2CH{=}CH_2)(CNBu^t)_2\}_2(\mu\text{-}Cl)]Cl$ (**10a**, Scheme 3), while the major one (85%) (**10b**) was found to be the asymmetric isomer depicted in Scheme 3 and was fully characterized by X-ray methods (vide infra). The ^{1}H NMR of **10b** showed broad signals at room temperature, while a well-defined spectrum was obtained on cooling. A complete spectroscopic NMR study including H,H−COSY, ^{1}H,^{13}C−HETCOR, and

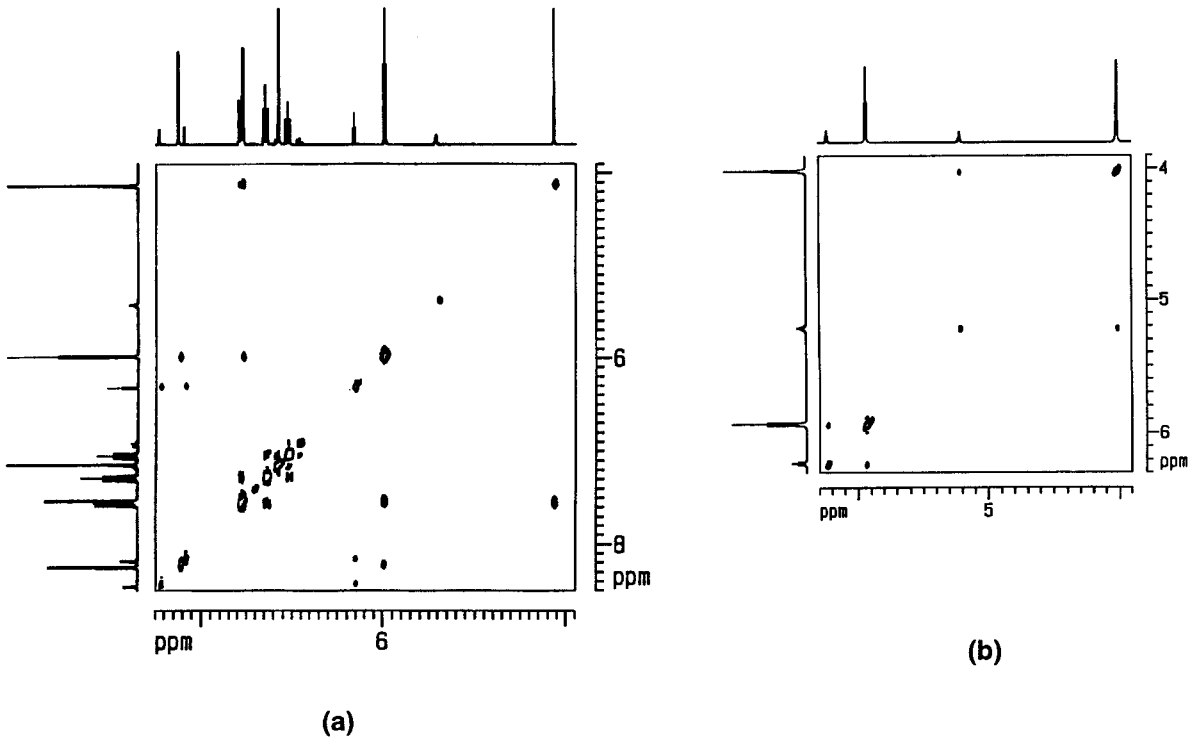

Figure 4. Phase-sensitive (a) NOESY and (b) ROESY spectra of [{Ir(μ-Pz)(CNBu^t)$_2$}$_2$(Cl)(η^1-CH_2Ph)] (**5a** and **5b**), showing the cross-peaks due to proximity effects (positive peaks), and the exchange of the pyrazolate and CH_2R groups of both species (negative peaks), respectively.

Scheme 3

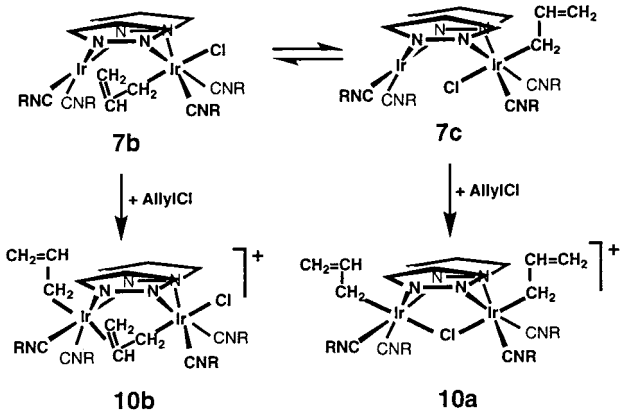

Scheme 4

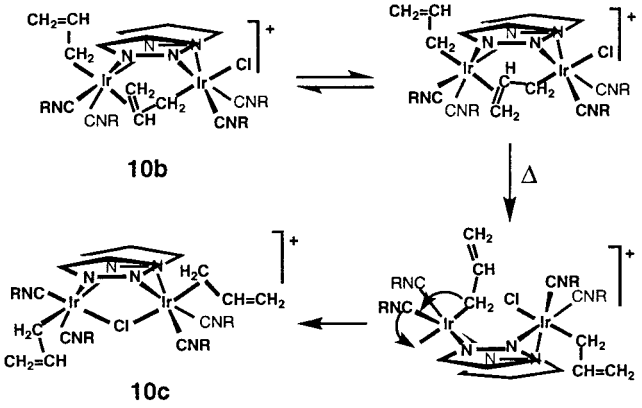

ROESY experiments, allowed us to conclude that in **10b** one allyl group was η^1-bonded to one iridium atom and the other allyl group was bridging, η^1-bonded to the second iridium and coordinated through the double C=C bond to the first one, as found in the solid state. The unsymmetric coordination of the allyl group as a σ,π-bonded propenyl bridge, evidenced for the frozen structure, is quite uncommon. Indeed, only two crystal structures of platinum complexes with σ,π-bonded propenyl bridges have been reported,[17] while symmetrical π-allyl bridging groups are well documented.[18] Most probably, the fluxionality observed for **10b** is related with the change of coordination of the two faces of the C=C bond to the second iridium atom (Scheme 4). Indeed, the room-temperature ^{1}H NMR spectrum of **10b** is more simple than at low temperature, as if the averaged species possesses a plane of symmetry bisecting the dihedral angle between the two pyrazolate rings.

Complexes **10a** and **10b** do not interconvert. Moreover, while **10a** remained unchanged, complex **10b** evolved into **10c** on heating above room temperature. The chemical transformation, quantitative by NMR, corresponded to an isomerization of **10b** into the nonsymmetric stereoisomer of **10a** containing a chloride-bridging ligand (Scheme 4).

Complex **10c** was found to be a 1:1 electrolyte in acetone. The lack of symmetry of the cation was evident from the observation of distinct signals for all protons and carbons in the ^{1}H and ^{13}C{^{1}H} NMR spectra. In addition, the two inequivalent η^1-CH_2CH=CH_2 groups were terminal and σ-bonded to the iridium atoms, as deduced from the similarity of the chemical shifts in the ^{13}C{^{1}H} NMR spectrum to those of **10a**. Moreover, these allyl groups are in a relative *transoid* disposition, which was corroborated by the NOESY spectrum, since only

(17) Raper, G.; McDonald, W. S. *J. Chem. Soc., Dalton Trans.* **1972**, 265.

(18) (a) Kurosawa, H.; Hirako, K.; Natsume, S.; Ogoshi, S.; Kanehisa, N.; Kai, Y.; Sakaki, S.; Takeuchi, K. *Organometallics* **1996**, *15*, 2089. (b) Werner, H. *Adv. Organomet. Chem.* **1981**, *19*, 155.

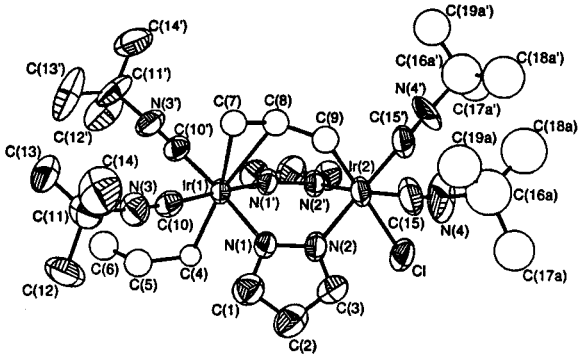

Figure 5. ORTEP molecular drawing (40% probability ellipsoids) of the cation of complex **10b** showing the distribution of ligands and the labeling scheme used. Only one set of the disordered ligands is shown. The molecule exhibits a crystallographic imposed symmetry plane through the iridium and Cl(1) atoms; primed atoms are related to the unprimed ones by the symmetry transformation $x, -y - 1/2, z$.

Table 1. Selected Bond Lengths (Å) and Angles (deg) for $[(CNBu^t)_2(\eta^1\text{-}CH_2CH{=}CH_2)Ir(\mu\text{-}Pz)_2(\eta^1,\eta^2\text{-}\mu\text{-}CH_2CH{=}CH_2)Ir(Cl)(CNBu^t)_2]Cl$ (10b)[a]

		Ir(2)−Cl(1)	2.480(5)
Ir(1)−N(1)	2.060(10)	Ir(2)−N(2)	2.075(11)
Ir(1)−C(4)	2.169(15)	Ir(2)−C(9)	2.132(18)
Ir(1)−C(7)	2.47(2)		
Ir(1)−C(8)	2.51(2)		
Ir(1)−C(10)	1.925(15)	Ir(2)−C(15)	1.949(19)
N(1)−Ir(1)−N(1′)	92.0(6)	Cl(1)−Ir(2)−N(2)	89.4(3)
N(1)−Ir(1)−C(4)	81.0(6)	Cl(1)−Ir(2)−C(9)	172.2(8)
N(1)−Ir(1)−CG[b]	93.7(6)	Cl(1)−Ir(2)−C(15)	91.8(4)
N(1)−Ir(1)−C(10)	89.5(5)	N(2)−Ir(2)−N(2′)	91.4(6)
N(1)−Ir(1)−C(10′)	175.2(5)	N(2)−Ir(2)−C(9)	86.0(7)
N(1′)−Ir(1)−C(4)	91.7(6)	N(2)−Ir(2)−C(15)	91.3(6)
N(1′)−Ir(1)−CG[b]	94.2(6)	N(2)−Ir(2)−C(15′)	177.0(6)
C(4)−Ir(1)−CG[b]	172.9(6)	N(2′)−Ir(2)−C(9)	97.0(7)
C(4)−Ir(1)−C(10)	84.0(6)	C(9)−Ir(2)−C(15)	82.1(7)
C(4)−Ir(1)−C(10′)	94.4(6)	C(9)−Ir(2)−C(15′)	92.5(8)
CG[b]−Ir(1)−C(10)	90.3(6)	C(15)−Ir(2)−C(15′)	85.9(10)
CG[b]−Ir(1)−C(10′)	90.8(6)		
C(10)−Ir(1)−C(10′)	88.7(8)		

[a] Primed atoms are related to the unprimed ones by a symmetry plane (symm transf: $x, -y - 1/2, z$). [b] CG represents the centroid of the C(7)−C(8) double bond.

three positive cross-peaks between the $H^{3,5}$ protons of the pyrazolate rings and the CH_2 protons of the allyl ligands were observed. Therefore, one allyl ligand is *cis* to both pyrazolate and *trans* to the chloride bridging ligand, while the other allyl moiety is *cis* to one pyrazolate but *trans* to the other.

The X-ray crystal structure analysis of **10b** (Figure 5) confirms the presence of the bridging σ,π-bonded propenyl ligand, for which there is not a fully characterized precedent in iridium and rhodium chemistry. Selected bond distances are collected in Table 1. The molecular structure shows two iridium atoms bridged by two exobidentate pyrazolate groups and by one allyl ligand, σ-bonded to Ir(2) and π-bonded to Ir(1) through the C=C bond. Both metals exhibit slightly distorted octahedral geometries, with an intermetallic separation of 3.8397(9) Å. Although the bridging and terminal propenyl ligands are involved in a situation of static disorder (see Experimental Section), the molecular structural determination clearly confirms the asymmetric coordination of the bridging ligand, η^1 to Ir(2) and η^2 to Ir(1). The long Ir−Cl bond distance, 2.480(5) Å, is in agreement wit the high structural *trans* influence of the σ-bonded carbon C(9), and the similar Ir(1)−C bond distances to C(8) and C(9), 2.47 and 2.51(2) Å, corroborate the σ,π-coordination of the bridging allyl ligand. Unfortunately, the geometric restraints needed to deal with the crystallographic disorder, applied to the C−C bond distances and angles, hinder any comparison within the C(7)−C(9) propenyl ligand.

Discussion

In this paper we show rare nonphotochemical reactions of dinuclear iridium complexes with activated alkyl chlorides leading to a variety of functionalized organoalkyldiiridium compounds. These dinuclear oxidative-addition reactions produce an already known type of metal−metal bonded diiridium(II) complexes in a first step and bis(alkyl)diiridium(III) complexes by further reaction of some of them with alkyl chlorides. Interestingly, some diiridum(II) complexes are in chemical equilibrium with the corresponding valence isomer Ir(I)−Ir(III) complexes in solution. The state of the equilibrium is determined by the nature of the halide ligand and the organic group on the iridium atoms. The influence of the halide on the equilibrium is exemplified by complexes **5** and **6**, which differ on the halide ligand. The Ir(II)−Ir(II) metal−metal bonded species and the Ir(I)−Ir(III) mixed-valence complex are found to be in equilibrium for the chloride complex **5**. However, addition of iodide shifts the equilibrium to the diiridium(II) complex **6**. A similar trend was also observed for the heterodinuclear complexes $[\{(\eta^6\text{-}p\text{-cymene})Ru(\mu\text{-}Pz)_2Ir(CO)_2\}X]$ (X = Cl, Br, I).[19] Regarding the influence of the organic group of the type $-CH_2R$ on the equilibrium, the III/I isomer is more favored for R = $CH{=}CH_2$, Ph than for R = COMe, CO_2Me. The incorporation of a methyl group at the α-carbon (R = $CH(Me)CO_2Me$) does not produce any appreciable effect. The main difference between these two groups is the stronger electron-withdrawing character of the carbonyl versus the C=C groups. A plausible interpretation for the influences of the halide and organic groups in the X−Ir−Ir−R moiety on the stabilization of the Ir(I)−Ir(III) isomer involves a polarization of the Ir−Ir bond determined by the nature of the X and R groups bonded in *trans* position. The more electronegative the halogenide, the more polarized the metal−metal bond, favoring the mixed-valence species. However, the result of this inductive effect can be blocked by electron-withdrawing organic groups on the second iridium atom, which in turn favors the diiridium(II) isomer.

The access to bis(alkyl)diiridium(III) complexes by reaction of diiridium(II) compounds with chloroalkanes is only possible for those that are able to isomerize to a detectable mixed-valence Ir(I)−Ir(III) complex. This suggests that the reactions of **5** and **7** reported herein occur with the species possessing an Ir(I) center that can undergo oxidative-addition of a second molecule of RCH_2Cl. Therefore, the diiridium(II) compounds and the mixed-valence Ir(I)−Ir(III) complex species not only are valence isomers but fall into the category of *tautomers*,

(19) Carmona, D.; Ferrer, J.; Mendoza, A.; Lahoz, F. J.; Reyes, J.; Oro, L. A. *Angew. Chem., Int. Ed. Engl.* **1991**, *30*, 1171.

and therefore, the process could be called a "*dinuclear valence-tautomerism*". However, the term valence-tautomerism has been used to describe internal metal−ligand electron transfer (valence tautomers) in mononuclear complexes.[20] As the mixed-valence tautomer reacts, the equilibrium regenerates this active species, and the reactions eventually go to completion.

Regarding the species in the tautomeric equilibria, we have been able to detect only a single conformer of the mixed-valence Ir(I)−Ir(III) species, namely, that possessing the organic fragment in the pocket of the complex (for example **5b** in Scheme 2). Most probably, the unobserved conformer (**5c**, Scheme 2) exists also in solution but in a percentage under the limit of detection of the NMR and could be the responsible for further reactions of **5** with a second molecule of chloro derivative to account for the structure of the products (**8** and **9**). Interestingly, the reaction of the allyl complex **7** with allyl chloride provides a unique case in which the two isomers coming from both conformers are observed (Scheme 3). Most probably, the isomer **10b** comes from the tautomer (**7b**) observed in the NMR spectrum, while **10a** comes from the **7c** conformer. Assuming an anchimeric effect and S_N2 mechanism for the second oxidative-addition reaction, both the chloride and allyl ligands could donate electronic density to the iridium undergoing the reaction, and therefore the speed of these reactions would become alike, producing both isomers in a ratio similar to those found in other conformational equilibria.[15]

The isomer **10b** with the bridging allyl ligand is a rare binuclear compound with an asymmetric allyl bridging ligand in which the C═C bond is localized. Moreover, this is a kinetic product for the addition of allyl chloride to **7**, since an isomerization takes place on heating to render the thermodyamic product **10c**, which contains the bridging chloride. A simple mechanism for this isomerization involves the rupture of the π-Ir−C═C bond, followed by the inversion of the six-membered metallacycle. This facilitates the access of the chloride to both iridium atoms becoming a bridging ligand, which produces the migration of one isocyanide from an equatorial to the axial position.

Experimental Section

Starting Materials and Physical Methods. All reactions were carried out under argon using standard Schlenk techniques. [{Ir(μ-Pz)(CNBu^t)$_2$}$_2$] (**1**) was prepared according to literature methods.[11] The organochlorinated compounds were distilled under argon prior to use. Solvents were dried and distilled under argon by standard methods. Pure complex **1** gives yellow-orange solutions in dried and deoxygenated solvents; otherwise purple or blue solutions were obtained. The new complexes described herein are light-sensitive and should be stored in the dark. The formulas of the hydrates, complexes **8**−**10**, are indicated with the analytical data, and the water of crystallization was observed at 1.56 ppm in $CDCl_3$ and at 2.81 and 2.84 ppm in acetone-d_6 in their ^{1}H NMR spectra. Physical measurements were carried out on the apparatus described in the preceding paper. NOE experiments were carried out using the standard CYCLENOE pulse sequence on the Varian spectrometer. The phase-sensitive NOESY and ROESY experiments were carried out with 512 FIDs, and the mixing times were optimized in the range of 0.4−1 s on the Bruker spectrometer.

Preparation of the Complexes. [(CNBu^t)$_2$(Cl)Ir(μ-Pz)$_2$Ir(η^1-CH$_2$COMe)(CNBu^t)$_2$] (2). Chloroacetone (20 μL, 0.25 mmol) was added to a solution of [{Ir(μ-Pz)(CNBu^t)$_2$}$_2$] (**1**) (200 mg, 0.23 mmol) in benzene (5 mL). After 30 min, the resulting pale yellow solution was carefully layered with hexane (20 mL) and allowed to stand 2 days in the darkness. The resulting pale yellow microcrystals were separated by decantation, washed with cold hexane (2 × 5 mL), and vacuum-dried. Yield: 200 mg (90%). Anal. Calcd for $C_{29}H_{47}N_8ClOIr_2$: C, 36.91; H, 5.02; N, 11.87. Found: C, 36.72; H, 5.29; N, 11.54. IR (toluene, cm^{-1}): ν(CN) 2179 (s), 2137 (s); ν(CO) 1641 (m). ^{1}H NMR (rt, acetone-d_6): δ 7.54 (d, 2.1 Hz, 2H, H^{3}Pz), 7.49 (d, 2.1 Hz, 2H, H^{5}Pz), 5.92 (t, 2H, H^{4}Pz), 3.46 (s, 2H, C*H*$_2$COMe), 2.32 (s, 3H, CH$_2$CO*Me*), 1.51 and 1.50 (s, 2 × 18H, CNBu^t). ^{13}C{^{1}H} NMR (rt, acetone-d_6): δ 208.3 (CO), 135.4 (C^{3}Pz), 132.1 (br) and 122.7 (br) (CN), 133.6 (C^{5}Pz), 104.0 (C^{4}Pz), 58.4 and 57.9 (*C*−(CH$_3$)$_3$), 31.5 and 31.0 (C−(*C*H$_3$)$_3$), 14.1 (CH$_2$CO*Me*), −5.4 (*C*H$_2$COMe). MS (FAB$^+$, acetone, *m*/*z*): 943, 7% (M + H$^+$); 907, 70% (M − Cl$^+$).

[(CNBu^t)$_2$(Cl)Ir(μ-Pz)$_2$Ir(η^1-CH$_2$CO$_2$Me)(CNBu^t)$_2$] (3) was prepared as yellow microcrystals as described for **2** starting from [{Ir(μ-Pz)(CNBu^t)$_2$}$_2$] (**1**) (129 mg, 0.15 mmol) and methylchloroacetate (14 μL, 0.15 mmol). Yield: 115 mg (80%). Anal. Calcd for $C_{29}H_{47}N_8ClO_2Ir_2$: C, 36.30; H, 4.94; N, 11.68. Found: C, 36.09; H, 4.54; N, 11.50. IR (toluene, cm^{-1}): ν(CN) 2187 (s), 2144 (s); ν(CO) 1679 (m). ^{1}H NMR (rt, C_6D_6): δ 8.20 (d, 2.0 Hz, 2H, H^{3}Pz), 7.63 (d, 2.0 Hz, 2H, H^{5}Pz), 5.94 (t, 2H, H^{4}Pz), 3.71 (s, 3H, CH$_2$CO$_2$*Me*), 3.53 (s, 2H, C*H*$_2$CO$_2$Me), 1.84 and 1.22 (s, 2 × 18H, CNBu^t). ^{13}C{^{1}H} NMR (rt, C_6D_6) δ: 181.2 (CO), 136.3 (C^{3}Pz), 135.4 (br) and 125.2 (br) (CN), 136.3 (C^{5}Pz), 104.6 (C^{4}Pz), 57.8 and 57.2 (*C*−(CH$_3$)$_3$), 49.7 (CH$_2$-CO$_2$*Me*), 31.6 and 31.2 (C−(*C*H$_3$)$_3$), −2.8 (*C*H$_2$CO$_2$Me). MS (FAB$^+$, acetone, *m*/*z*): 959, 55% (M$^+$); 907, 10% (M − Cl$^+$); 941, 100% (M − Cl + H$_2$O$^+$).

(±)-[(CNBu^t)$_2$(Cl)Ir(μ-Pz)$_2$Ir{η^1-CH(Me)CO$_2$Me}-(CNBu^t)$_2$] (4) was prepared as yellow needles as described for **2** starting from [{Ir(μ-Pz)(CNBu^t)$_2$}$_2$] (**1**) (200 mg, 0.23 mmol) and (−)-methyl(S)-2-chloropropionate (26 μL, 0.23 mmol). Yield: 149 mg (65%). Anal. Calcd for $C_{30}H_{49}N_8O_2ClIr_2$: C, 37.01; H, 5.07; N, 11.51. Found: C, 37.31; H, 4.95; N, 11.61. IR (diethyl ether, cm^{-1}): ν(CN) 2181 (s), 2139 (s), 2080 (sh), 2052 (m). ^{1}H NMR (rt, C_6D_6): δ 8.22 (d, 2.0 Hz, 1H), 8.20 (d, 2.0 Hz, 1H), 8.08 (d, 1.7 Hz, 1H) and 7.69 (d, 1.8 Hz, 1H) H$^{3,3',5,5'}$Pz, 6.00 (t, 1H) and 5.95 (t, 1H) H$^{4,4'}$Pz, 4.05 (q, 6.8 Hz, 1H, C*H*(Me)CO$_2$Me), 3.69 (s, 3H, CH(Me)CO$_2$*Me*), 2.07 (d, 6.8 Hz, 3H, CH(*Me*)CO$_2$Me), 1.24, 1.24, 1.13, and 1.04 (s, 4 × 9H, CNBu^t). ^{13}C{^{1}H} NMR (rt, C_6D_6): δ 182.9 (CO), 136.6, 136.4, 134.3 and 134.1 (C$^{3,3',5,5'}$Pz), 138.7, 138.5, 123.6 (br) and 123.3 (br) (CN), 104.6 and 104.4 (C$^{4,4'}$Pz), 58.2 and 57.0 (*C*-(CH$_3$)$_3$), 49.6 (CH(Me)CO$_2$*Me*), 31.8, 31.0 and 30.8 (C−(*C*H$_3$)$_3$), 22.9 (CH(*Me*)CO$_2$Me), 7.0 (*C*H(Me)CO$_2$Me). MS (FAB$^+$, acetone, *m*/*z*): 973, 35% (M$^+$); 937, 100% (M − Cl$^+$). Λ_M (5.02 10^{-4} M in acetone): 2 S cm^2 mol^{-1}.

[{Ir(μ-Pz)(CNBu^t)$_2$}$_2$(Cl)(η^1-CH$_2$Ph)] (5). To a solution of [{Ir(μ-Pz)(CNBu^t)$_2$}$_2$] (**1**) (200 mg, 0.23 mmol) in benzene (5 mL) was added benzyl chloride (27 μL, 0.23 mmol) in the darkness. After 30 min, the reaction mixture was carefully layered with pentane (20 mL) and then left in the refrigerator overnight. The resulting orange crystals were separated by decantation, washed with pentane, and dried under vacuum. Yield: 230 mg (82%). Anal. Calcd for $C_{33}H_{49}N_8ClIr_2$·0.5 C_6H_6: C, 42.57; H, 5.15; N, 11.02. Found: C, 42.23; H, 5.11; N, 11.13. IR (diethyl ether, cm^{-1}): ν(CN) 2177 (s), 2133 (s), 2091 (sh), 2039 (m). ^{1}H NMR (rt, C_6D_6) (major isomer): δ 8.27 (d, 2.0 Hz, 2H, H^{3}Pz), 7.54 (d, 2.0 Hz, 2H, H^{5}Pz), 7.58 (d, 7.6 Hz, 2H, H^{o}Ph), 7.29 (t, 7.6 Hz, 2H, H^{m}Ph), 7.05 (t, 1H, H^{p}Ph), 5.99 (t, 2H, H^{4}Pz), 4.15 (s, 2H, CH$_2$), 1.24 and 0.94 (s, 2 × 18H, CNBu^t); (minor isomer, data obtained from the COSY spectrum): δ 8.48 (d, 2.2 Hz, 2H, H^{3}Pz), 8.19 (d, 2.2 Hz, 2H,

(20) (a) Roux, C.; Adams, D. M.; Itié, J. P.; Polian, A.; Hendrickson, D. N.; Verdaguer, M. *Inorg. Chem*. **1996**, *35*, 2846.

H^5Pz), 7.21 (2H, H^oPh), 7.05 (2H, H^mPh), 6.99 (1H, H^pPh), 6.33 (t, 2H, H^4Pz), 5.44 (s, 2H, CH_2), 1.04 and 0.88 (s, 2 × 18H, CNBu^t). MS (FAB$^+$, acetone, *m*/*z*): 977, 100% (M^+). Λ_M (4.99 10^{-4} M in acetone): 12 S cm^2 mol^{-1}.

[(CNBu^t)$_2$(I)Ir(μ-Pz)$_2$Ir(η^1-CH$_2$Ph)(CNBu^t)$_2$] (6). To an orange solution of [{Ir(μ-Pz)(CNBu^t)$_2$}$_2$(Cl)(η^1−CH$_2$Ph)] (**5**) (90 mg, 0.09 mmol) in acetone (4 mL) was added solid KI (30 mg, 0.18 mmol). After stirring for 2 h the resulting suspension was evaporated to dryness and extracted with dichloromethane to remove the KCl formed. Concentration of the orange solution and crystallization with hexane gives orange microcrystals of **7**, which were separated by decantation and vacuum-dried. Yield: 75 mg (76%). Anal. Calcd for $C_{33}H_{49}N_8IIr_2$: C, 37.07; H, 4.62; N, 10.48. Found: C, 37.27 H, 4.56; N, 10.34. IR (CH_2Cl_2, cm^{-1}): ν(CN) 2214 (s), 2183 (s); ν(Ph) 1634 (m). ^{1}H NMR (rt, acetone-d_6): δ 7.62 (d, 2.4 Hz, 2H, H^3Pz), 7.42 (d, 2.0 Hz, 2H, H^5Pz), 7.34 (d, 7.3 Hz, 2H, H^oPh), 7.16 (t, 7.3 Hz, 2H, H^mPh), 6.91 (t, 1H, H^pPh), 5.91 (t, 2H, H^4Pz), 3.75 (s, 2H, CH_2), 1.46 and 1.37 (s, 2 × 18H, CNBu^t). ^{13}C{^{1}H} NMR (rt, acetone-d_6): δ 140.2 (C^3Pz), 133.1 (C^5Pz), 154.8, 128.2, 127.2 and 121.5 (Ph), 104.1 (C^4Pz), 58.0 and 59.1 (C−(CH$_3$)$_3$), 31.4 and 30.7 (C−(CH_3)$_3$), 2.8 (CH_2Ph).

[{Ir(μ-Pz)(CNBu^t)$_2$}$_2$(Cl)(η^1-CH$_2$CH=CH$_2$)] (7) was prepared as orange crystals as described for **5** starting from [{Ir(μ-Pz)(CNBu^t)$_2$}$_2$] (**1**) (129 mg, 0.15 mmol) and allyl chloride (12 μL, 0.15 mmol). Yield: 112 mg (80%). Anal. Calcd for $C_{29}H_{47}N_8ClIr_2$: C, 37.55; H, 5.11; N, 12.08. Found: C, 37.52; H, 5.04; N, 12.13. IR (toluene, cm^{-1}): ν(CN) 2179 (s), 2137 (s), 2075 (sh), 2044 (sh); ν(C=C) 1610 (m). ^{1}H NMR (233 K, toluene-d_8) major isomer: δ 8.20 (d, 1.8 Hz, 2H, H^3Pz), 7.49 (d, 1.8 Hz, 2H, H^3Pz), 6.82 (m, 1H, η^1-CH$_2$C*H*=CH$_2$), 5.93 (t, 2H, H^4Pz), 5.30 (dd, 16.5 and 2.7 Hz, 1H) and 4.97 (dd, 9.6 and 2.7 Hz, 1H) (η^1-CH$_2$CH=C*H*$_2$), 3.63 (d, 8.7 Hz, 2H, η^1-C*H*$_2$-CH=CH$_2$), 1.15 and 0.98 (s, 2 × 9H, CNBu^t); minor isomer: δ 8.46 (d, 2.4 Hz, 2H, H^3Pz), 8.10 (d, 2.4 Hz, 2H, H^5Pz), 6.46 (m, 1H, η^1-CH$_2$C*H*=CH$_2$), 6.32 (t, 2H, H^4Pz), 5.08 (dd, 16.5 and 2.7 Hz, 1H) and 4.89 (dd, 9.9 and 3.0 Hz, 1H) (η^1-CH$_2$CH=C*H*$_2$), 4.66 (d, 8.4 Hz, 2H, η^1-C*H*$_2$CH=CH$_2$), 1.03 and 0.95 (s, 2 × 9H, CNBu^t). ^{13}C{^{1}H} NMR (233K, toluene-d_8) mayor isomer: δ 136.7 (C^3Pz), 132.4 (C^5Pz), 104.6 (C^4Pz); 57.6 and 56.8 (C−(CH$_3$)$_3$), 31.6 and 30.9 (C−(*C*H$_3$)$_3$); 151.6 (η^1-CH$_2$*C*H=CH$_2$), 102.2 (η^1-CH$_2$CH=*C*H$_2$), 2.9 (η^1-*C*H$_2$CH=CH$_2$). MS (FAB$^+$, acetone, *m*/*z*): 927, 100% (M + H$^+$).

[{Ir(μ-Pz)(η^1−CH$_2$Ph)(CNBu^t)$_2$}$_2$(μ-Cl)]Cl (8). Benzyl chloride (12 μL, 0.10 mmol) was added to a solution of [{Ir(μ-Pz)(CNBu^t)$_2$}$_2$(Cl)(η^1-CH$_2$Ph)] (**5**) (97 mg, 0.10 mmol) in benzene (3 mL) and carefully layered with pentane (15 mL) overnight in the darkness. The resulting white crystals were separated by decantation, washed with diethyl ether, and dried under vacuum. Yield: 116 mg (92%). Anal. Calcd for $C_{40}H_{56}N_8Cl_2Ir_2$·2H$_2$O: C, 42.13; H, 5.21; N, 9.98. Found: C, 42.57; H, 5.13; N, 9.87. IR (CH_2Cl_2, cm^{-1}): ν(CN) 2220 (s), 2187 (s). ^{1}H NMR (rt, $CDCl_3$): δ 7.64 (d, 2.3 Hz, 4H, $H^{3,5}$Pz), 7.23 (d, 7.2 Hz, 4H, H^oPh), 7.14 (t, 7.2 Hz, 4H, H^mPh), 7.04 (t, 2H, H^pPh), 6.31 (t, 2H, H^4Pz), 3.46 (s, 4H, CH_2), 1.08 (s, 36H, CNBu^t). ^{13}C{^{1}H} NMR (rt, $CDCl_3$): δ 139.7 ($C^{3,5}$Pz), 149.8, 128.5, 128.4 and 125.0 (Ph), 106.8 (C^4Pz), 58.7 (C−(CH$_3$)$_3$), 29.9 (C−(*C*H$_3$)$_3$), 8.8 (CH_2Ph). MS (FAB$^+$, CH_2Cl_2, *m*/*z*): 1069, 100% (M^+). Λ_M (4.99 10^{-4} M in acetone): 89 S cm^2 mol^{-1}.

[(CNBu^t)$_2$(η^1−CH$_2$Ph)Ir(μ-Pz)$_2$(μ-Cl)Ir(η^1-CH$_2$CO$_2$CH$_3$)(CNBu^t)$_2$]Cl (9) was prepared as described for **8** starting from [{Ir(μ-Pz)(CNBu^t)$_2$}$_2$(Cl)(η^1-CH$_2$Ph)] (**5**) (68 mg, 0.07 mmol) and methylchloroacetate (6.5 μL, 0.07 mmol) to give white microcrystals. Yield: 70 mg (92%). Anal. Calcd for $C_{36}H_{54}N_8O_2Cl_2Ir_2$·2H$_2$O: C, 38.53; H, 5.20; N, 9.98. Found: C, 38.00; H, 5.30; N, 9.75. IR (CH_2Cl_2, cm^{-1}): ν(CN) 2224 (s), 2193 (s); ν(CO) 1713 (m). ^{1}H NMR (rt, $CDCl_3$): δ 7.69 (d, 2.2 Hz, 2H, H^3Pz), 7.62 (d, 2.2 Hz, 2H, H^5Pz), 7.19 (m, 4H, $H^{o,m}$Ph), 7.09 (t, 6.8 Hz, 1H, H^pPh), 6.26 (t, 2H, H^4Pz), 3.64 (s, 3H, CO_2CH_3), 3.45 (s, 2H, CH_2Ph), 2.75 (s, 2H, $CH_2CO_2CH_3$), 1.44 and 1.28 (s, 2 × 18H, CNBu^t). ^{13}C{^{1}H} NMR (rt, $CDCl_3$): δ 180.4 (CO), 140.1 and 139.7 ($C^{3,5}$Pz), 149.8, 128.7, 128.4, and 125.3 (Ph), 106.9 (C^4Pz), 59.2 and 59.0 (*C*-(CH$_3$)$_3$), 50.9 (CO_2CH_3), 30.4 and 30.1 (C−(*C*H$_3$)$_3$), 8.8 (CH_2Ph), 1.6 ($CH_2CO_2CH_3$). MS (FAB$^+$, CH_2Cl_2, *m*/*z*): 1050, 100% (M^+). Λ_M (4.99 10^{-4} M in acetone): 89 S cm^2 mol^{-1}.

Chart 2

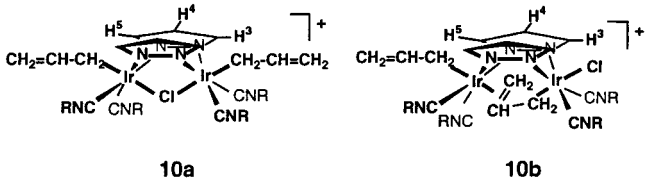

10a **10b**

Chart 3

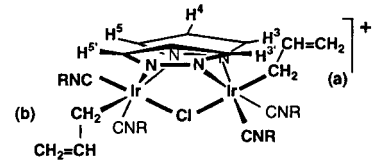

[{Ir(μ-Pz)(CNBu^t)$_2$}$_2$(Cl)(η^1-CH$_2$CH=CH$_2$)$_2$]Cl (10a, 10b) were prepared as described for **8** starting from [{Ir(μ-Pz)(CNBu^t)$_2$}$_2$(Cl)(η^1-CH$_2$CH=CH$_2$)] (**6**) (102 mg, 0.11 mmol) and allyl chloride (10 μL, 0.12 mmol) to give white microcrystals of a mixture of **10a**/**10b** in 15:85 molar ratio (Chart 2). Yield: 88 mg (80%). Anal. Calcd for $C_{32}H_{52}N_8Cl_2Ir_2$·2H$_2$O: C, 36.95; H, 5.43; N, 10.77. Found: C, 37.04; H, 5.30; N, 10.92. IR (CH_2Cl_2, cm^{-1}): ν(CN) 2218 (s), 2187 (s); ν(C=C) 1612 (m). MS (FAB$^+$, CH_2Cl_2, *m*/*z*): 969, 100% (M^+). Pure **10b** as monocrystals was obtained by recrystallization of the above mixture from dichloromethane/diethyl ether. Spectroscopic data were assigned from H,H-COSY, H,H-NOESY, and H,C-HETCOR. (**10a**) ^{1}H NMR (233 K, acetone-d_6): δ 7.88 (d, 2.1 Hz, 4H, $H^{3,5}$-Pz), 6.39 (t, 2H, H^4Pz), 6.41 (m, 2H, η^1-CH$_2$C*H*=CH$_2$), 5.31 (dd, 16.8 and 1.8 Hz, 2H) and 5.03 (dd, 9.9 and 2.1 Hz, 2H) (η^1-CH$_2$CH=C*H*$_2$), 2.97 (d, 8.4 Hz, 4H, η^1-C*H*$_2$CH=CH$_2$), 1.61 (s, 36H, CNBu^t). ^{13}C{^{1}H} NMR (233 K, acetone-d_6): δ 140.3 ($C^{3,5}$-Pz), 107.6 (C^4Pz); 59.6 (*C*-(CH$_3$)$_3$), 30.1 (C−(*C*H$_3$)$_3$); 147.3 (η^1-CH$_2$*C*H=CH$_2$), 110.7 (η^1-CH$_2$CH=*C*H$_2$), 9.17 (η^1-*C*H$_2$CH=CH$_2$). **(10b)** ^{1}H NMR (233 K, acetone-d_6): δ 7.87 (d, 2.1 Hz, 1H) and 7.73 (d, 2.1 Hz, 1H) ($H^{3,3'}$Pz), 7.64 (d, 2.1 Hz, 1H) and 7.47 (d, 2.1 Hz, 1H) ($H^{5,5'}$Pz), 6.27 (t, 1H) and 6.24 (t, 1H) ($H^{4,4'}$Pz); 6.38 (m, 1H, η^1-CH$_2$C*H*=CH$_2$), 5.13 (dd, 16.8 and 1.8 Hz, 1H) and 4.97 (dd, 9.6 and 2.1 Hz, 1H) (η^1-CH$_2$CH=C*H*$_2$), 2.77 (t, 9.0 Hz, 1H) and 2.41 (t, 9.0 Hz, 1H) (η^1-C*H*$_2$CH=CH$_2$); 5.55 (m, 1H, μ-CH$_2$C*H*=CH$_2$), 5.52 (m, 1H) and 4.92 (m, 1H) (μ-CH$_2$CH=C*H*$_2$), 3.82 (dd 16.5 and 2.0 Hz, 1H) and 1.79 (d, 16.5 Hz, 1H) (μ-C*H*$_2$CH=CH$_2$); 1.77, 1.67, 1.61, and 1.55 (s, 4 × 9H, CNBu^t). ^{13}C{^{1}H} NMR (233 K, acetone-d_6): δ 144.9 and 144.1 ($C^{3,3'}$Pz), 142.9 and 141.9 ($C^{5,5'}$Pz), 107.3 and 107.1 ($C^{4,4'}$-Pz); 60.4, 60.2, 59.2 and 59.1 (C−(CH$_3$)$_3$), 146.1 (η^1-CH$_2$*C*H=CH$_2$), 111.3 (η^1-CH$_2$CH=*C*H$_2$), 21.1 (η^1-*C*H$_2$CH=CH$_2$); 129.7 (μ-CH$_2$*C*H=CH$_2$), 86.2 (μ-CH$_2$CH=*C*H$_2$), −4.1 (μ-*C*H$_2$CH=CH$_2$).

[{Ir(μ-Pz)(η^1-CH$_2$CH=CH$_2$)(CNBu^t)$_2$}$_2$(μ-Cl)]Cl (10c). Heating a pure sample of **10b** in acetone-d_6 or in $CDCl_3$ at 60 °C in the NMR cavity for 2 h produces the complete transformation into **10c** (Chart 3). Complex **10c** was isolated as a white solid by crystallization, layering the acetone solution (0.5 mL) with diethyl ether (5 mL). Anal. Calcd for $C_{32}H_{52}N_8Cl_2Ir_2$·2H$_2$O: C, 36.95; H, 5.43; N, 10.77. Found: C, 37.04; H, 5.30; N, 10.92. IR (CH_2Cl_2, cm^{-1}): ν(CN) 2218 (s), 2187 (s); ν(C=C) 1606 (m). ^{1}H NMR (rt, $CDCl_3$): δ 7.55 (d, 1.8 Hz, 1H) and 7.53 (d, 2.4 Hz, 1H) ($H^{5,5'}$ Pz), 7.49 (d, 1.9 Hz, 1H) and 7.43 (d, 2.1 Hz, 1H) ($H^{3',3}$ Pz), 6.28 (t, 2.4 Hz, 1H) and 6.26 (t, 2.1 Hz, 1H) ($H^{4',4}$ Pz); 6.71 (m, 2H, CH$_2$C*H*=CH$_2$ a and b), 5.19 (dm, 16.8 Hz, 1H) and 4.97 (dd, 9.9 and 2.1 Hz, 1H) (η^1-CH$_2$CH=C*H*$_2$ a), 3.01 (t, 9.6 Hz, 1H) and 2.93 (t, 9.9 Hz, 1H) (C*H*$_2$CH=CH$_2$

Table 2. Crystallographic Data for $[(CNBu^t)_2(\eta^1\text{-}CH_2CH{=}CH_2)Ir(\mu\text{-}Pz)_2(\eta^1,\eta^2\text{-}\mu\text{-}CH_2CH{=}CH_2)Ir(Cl)(CNBu^t)_2]Cl$ (10b)

chem formula	$C_{32}H_{52}Cl_2Ir_2N_8{\cdot}CH_2Cl_2$
fw	1089.04
temp, K	293
cryst syst	monoclinic
space group	$P2_1/m$ (no. 11)
a, Å	13.0890(6)
b, Å	11.4237(7)
c, Å	15.3290(6)
β, deg	101.290(4)
V, Å^3	2247.7(2)
Z	2
$\rho_{(calcd)}$, g cm^{-3}	1.609
μ, mm^{-1}	6.182
θ range data collec, deg	1.9−25.0
no. of reflns collected	5153
no. of unique reflns	4169 ($R_{int} = 0.0503$)
no. of data/restraints/params	4169/47/227
$R(F)$ [$F^2 > 2\sigma(F^2)$][a]	0.0614
$wR(F^2)$ [all data][b]	0.1422

[a] $R(F) = \sum||F_o| - |F_c||/\sum|F_o|$, for 2434 observed reflections. [b] $wR(F^2) = (\sum[w(F_o^2 - F_c^2)^2]/\sum[w(F_o^2)^2])^{1/2}$.

a); 4.95 (dm, 16.8 Hz, 1H), 4.71 (dd, 9.9, 2.4 Hz, 1H) (CH_2-$CH{=}CH_2$ b), 2.90 (t, 9.3 Hz, 1H) and 2.53 (t, 9.3 Hz, 1H) (CH_2-$CH{=}CH_2$ b); 1.60, 1.57, 1.56 and 1.52 (s, 4 × 9H, $CNBu^t$). $^{13}C\{^1H\}$ NMR (rt, $CDCl_3$): δ 140.4, 139.3, 138.4, 138.2 ($C^{3,3',5,5'}$-Pz); 106.8, 106.7 ($C^{4,4'}$Pz); 59.5, 59.1, 59.1, 58.9 ($C{-}(CH_3)_3$); 30.7, 30.7, 30.6, 30.6 ($C{-}(CH_3)_3$); 147.6, 146.3 ($CH_2CH{=}CH_2$); 110.9, 108.3 ($CH_2CH{=}CH_2$); 8.9, 3.2 ($CH_2CH{=}CH_2$).

Crystal Structure Determination of Complex 10b. A summary of crystal data, intensity collection, and refinement parameters is reported in Table 2. A colorless irregular crystal was glued to a glass fiber and mounted on a Siemens-Stoe AED2 diffractometer with graphite-monochromated Mo Kα radiation ($\lambda = 0.71073$ Å). Cell constants were obtained from the least-squares fit on the setting angles of 100 reflections in the range $25° \le 2\theta \le 35°$. Data were collected at room temperature using the $\omega/2\theta$ scan method ($4° \le 2\theta \le 50°$; $-15 \le h \le 2$, $0 \le k \le 13$, $-18 \le l \le 18$). Three standard reflections were monitored every 55 min throughout the data collection; a decay of 11.4% was observed and consequently corrected according standard intensities. All data were corrected for Lorentz and polarization effects and for absorption using the ψ-scan method (min. and max. transm factors 0.1009 and 0.1273).[21]

The structures were solved by Patterson methods (SHELXS-97)[22] and Fourier techniques and refined by full-matrix least-squares on F^2 (SHELXL-97).[22] The dinuclear complex sits at both sides of a crystallographic mirror plane with the Ir(1), Ir(2), and Cl(1) atoms occupying special positions on the symmetry plane. The two allyl ligands (C(4)−C(6) terminal and C(7)−C(9) bridging) are not congruent with this plane, and they have been refined as two moieties disordered in the crystal (0.50 fixed occupancy). To prevent the atoms of these two disordered ligands from collapsing during refinement into the symmetry plane, geometric restraints were placed on the C−C bond distances (C−C 1.51(2), C═C 1.46(2), C···C 2.60(2) Å for the terminal allyl[23] and C−C 1.46(2), C═C 1.40(2), C···C 2.50(2) Å for the bridging allyl).[17] As the presence of this disorder involving the allylic ligands could be interpreted in terms of an erroneous selection of the spatial group, an alternative refinement with a symmetry reduction to the $P2_1$ space group was carried out; under this symmetry no convergence was obtained,[24] and the huge anisotropic displacement parameters obtained for the carbon atoms of the allylic ligands confirmed the existence of static disorder.

The *tert*-butyl group of one *tert*-butylisocyanide ligand was also found to be disordered: two moieties with equal occupancy were introduced in the refinement (C(16a)−C(19a) and C(16b)−C(19b); 0.50(4) refined occupancy). The bond distances and angles within both disordered moieties were restrained to common values, and a 3-fold symmetry was maintained within each set of atoms. A dichloromethane solvent molecule was also observed highly disordered; it was refined as three different models (and two more symmetry-generated) in the same spatial zone. Bond distances and angles were also restrained to the usual values for this molecule.[23] The sum of the refined occupancy factors was restrained to one, and two common isotropic displacement parameters were used: one for carbon atoms and a second one for chlorides.

Anisotropic displacement parameters were used in the last cycles of refinement for all nondisordered atoms, while isotropic ones were included for disordered groups. No attempt was made to include hydrogen atoms in the refinement. Atomic scattering factors, corrected for anomalous dispersion, were used as implemented in the refinement program. The calculated weighting scheme was $1/[\sigma^2(F_o^2) + (xP)^2 + yP]$, where $x = 0.0591$, $y = 4.7225$, and $P = (F_o^2 + 2F_c^2)/3$. Final agreements factors were $R(F) = 0.0614$ (2434 observed reflections, $F_o^2 < 2\sigma(F_o^2)$) and $wR(F^2) = 0.1422$. Largest peak and hole in the difference map were 1.451 (close to one iridium atom) and −0.972 e Å^{-3}.

Acknowledgment. The generous financial support from Dirección General de Enseñanaza Superior e Investigación (DGES) is gratefully acknowledged (Projects PB98-641 and PB94-1186).

Supporting Information Available: Full listings of crystallographic data, complete atomic coordinates, isotropic and anisotropic displacement parameters, and complete bond distances and angles for complex **10b**. This material is available free of charge via the Internet at http://pubs.acs.org.

OM000314V

(21) (a) *XPREP Program*, Rel. 5.03; Siemens Analytical X-ray Instruments, Inc.: Madison, WI, 1994. (b) North, A. C. T.; Phillips, D. C.; Mathews, F. S. *Acta Crystallogr., Sect. A* **1968**, *24*, 351.

(22) Sheldrick, G. M. *SHELX-97*; University of Göttingen: Germany, 1997.

(23) Allen, F. H.; Kennard, O. *Chem. Des. Automation News* **1993**, *8*, 31.

(24) Watkin, D. *Acta Crystallogr., Sect. A* **1994**, *50*, 411.